Am J Physiol Renal Physiol 315: F313–F322, 2018.
First published April 18, 2018; doi:10.1152/ajprenal.00065.2018.

RESEARCH ARTICLE

Chronic lithium treatment induces novel patterns of pendrin localization and expression

Nathaniel J. Himmel,[1] Yirong Wang,[1] Daniel A. Rodriguez,[1] Michael A. Sun,[1] and Mitsi A. Blount[1,2]

[1]*Renal Division, Department of Medicine, Emory University School of Medicine, Atlanta, Georgia; and* [2]*Department of Physiology, Emory University School of Medicine, Atlanta, Georgia*

Submitted 6 February 2018; accepted in final form 12 April 2018

Himmel NJ, Wang Y, Rodriguez DA, Sun MA, Blount MA. Chronic lithium treatment induces novel patterns of pendrin localization and expression. *Am J Physiol Renal Physiol* 315: F313–F322, 2018. First published April 18, 2018; doi:10.1152/ajprenal.00065.2018.—Prolonged lithium treatment is associated with various renal side effects and is known to induce inner medullary collecting duct (IMCD) remodeling. In animals treated with lithium, the fraction of intercalated cells (ICs), which are responsible for acid-base homeostasis, increases compared with renal principal cells (PCs). To investigate the intricacies of lithium-induced IMCD remodeling, male Sprague-Dawley rats were fed a lithium-enriched diet for 0,1, 2, 3, 6, 9, or 12 wk. Urine osmolality was decreased at 1 wk, and from 2 to 12 wk, animals were severely polyuric. After 6 wk of lithium treatment, approximately one-quarter of the cells in the initial IMCD expressed vacuolar H^+-ATPase, an IC marker. These cells were localized in portions of the inner medulla, where ICs are not normally found. Pendrin, a Cl^-/HCO_3^- exchanger, is normally expressed only in two IC subtypes found in the convoluted tubule, the cortical collecting duct, and the connecting tubule. At 6 wk of lithium treatment, we observed various patterns of pendrin localization and expression in the rat IMCD, including a novel phenotype wherein pendrin was coexpressed with aquaporin-4. These observations collectively suggest that renal IMCD cell plasticity may play an important role in lithium-induced IMCD remodeling.

acid-base homeostasis; acidosis; diabetes insipidus; lithium; pendrin

INTRODUCTION

Lithium is a drug commonly used in the treatment of bipolar disorder (36). Lithium also has beneficial effects on other central nervous system disorders, including stroke, multiple sclerosis, HIV-associated neurotoxicity, and Huntington's disease (7). However, chronic lithium therapy can result in various side effects of the renal, neurological, and endocrine systems (36). One such renal side effect is nephrogenic diabetes insipidus (NDI), in which patients present with polyuria, polydipsia, a reduced capacity to produce concentrated urine, and an insensitivity to vasopressin (25, 40). Approximately 40% of patients on prolonged lithium therapy develop NDI (25, 40), and in many of these cases, NDI cannot be reversed, rendering cessation of therapy not effective or advantageous to the patient (17). Treatment for lithium-induced NDI can include thiazide, amiloride, and/or acetazolamide; however, although great strides have been made in the efficacy of these treatments, side effects can still be problematic for patients (11). Furthermore, a complete understanding of the mechanisms underlying lithium-induced NDI has not been elucidated.

Under normal conditions, urine concentration is regulated by arginine vasopressin (AVP), which acts on the renal collecting duct to increase water absorption during hypovolemia or hypernatremia (26). AVP acts on the basolateral type 2 AVP receptor and ultimately leads to cAMP-mediated phosphorylation and subsequent membrane accumulation of aquaporin-2 (AQP2) in renal principal cells (18). Through the same mechanism, AVP also promotes phosphorylation and accumulation of the urea transporter, UT-A1, in inner medullary collecting duct (IMCD) cells, which contributes to the interstitial osmotic gradient of the inner medulla (IM), making it energetically favorable for water to be reabsorbed from the collecting duct (4). This is accomplished via the aforementioned accumulation of aquaporins, wherein water enters renal principal cells through AQP2 and exits into the interstitium via basolateral AQP3 and AQP4 (32). This process normally results in concentrated urine.

It has been shown that acute administration of lithium inhibits cAMP formation (30, 43), disrupting the above mentioned capacity of a cell to move AQP2 and UT-A1 to the apical membrane and thereby, the collecting duct's ability to concentrate urine. It has also been shown that with chronic lithium treatment, AQP2 and UT-A1 protein abundances are decreased, exacerbating this effect (5). Dysregulation of renal prostaglandins (35), altered purinergic signaling (55), and modifications of the phosphatidylinositol signaling pathway (19, 31, 49, 54), have also been implicated in lithium-induced NDI.

As a consequence of an inability to properly concentrate urine, lithium-induced NDI patients will often develop hyperchloremic acidosis (21). This is believed to manifest due to an inability to reabsorb HCO_3^- (33). Acid-base homeostasis is largely managed by renal intercalated cells, and final acid-base regulation occurs in the collecting duct, chiefly among two types of intercalated cells: type A and type B (2). Type A intercalated cells secrete H^+ via apical expression of vacuolar H^+-ATPase (V-ATPase), and reabsorb HCO_3^- through AE1, a band 3-like Cl^-/HCO_3^- exchanger (2, 20). In contrast, type B intercalated cells express V-ATPase basolaterally and intracellularly and secrete HCO_3^- via apically expressed pendrin, a Cl^-/HCO_3^- exchanger (48). A third type of intercalated cell,

Address for reprint requests and other correspondence: M. A. Blount, 338D Woodruff Memorial Bldg., 1639 Pierce Dr., Atlanta, GA 30322 (e-mail: mabloun@emory.edu).

termed non-A, non-B intercalated cells, expresses both V-ATPase and pendrin apically; yet the function of this cell type remains unknown (23, 47). While type A cells are found as deep as the initial portion of the IMCD, cells expressing pendrin are found only in the distal convoluted tubule, the cortical collecting duct, and the connecting tubule (47).

Lithium treatment is known to induce cellular remodeling of the collecting duct, eventually increasing the fraction of renal intercalated cells to renal principal cells (9, 12). During the early stages of lithium treatment, however, lithium induces proliferation in principal cells (8). Christensen et al. (8) concluded that apoptosis and principal-to-intercalated cell conversion are not suitable explanations for the eventual shift toward a higher fraction of intercalated cells, reporting that very few cells are apoptotic and that very few cells were observed to coexpress both principal and intercalated cell markers. de Groot et al. (10) have since described that a significant portion of proliferating cell nuclear antigen (PCNA)-positive principal cells are arrested in the G2 phase of cell division. These studies do not complete our understanding of IMCD remodeling, and it remains unclear what occurs during long-term treatment, and how this remodeling might relate to lithium-associated side effects.

In this study, we explored rat IMCD remodeling over 12 wk of lithium treatment. Herein, we detail remodeling of the IMCD in response to long-term lithium treatment-remodeling, which includes expression of a novel renal cell phenotype.

MATERIALS & METHODS

Animals. All animal protocols were approved by the Emory University Institutional Animal Care and Use Committee. Male-Sprague Dawley rats (Charles River; SAS SD, strain code 400) were fed either standard diet (containing 23% protein) supplemented with lithium carbonate (40 mmol/kg; Harlan Teklad, Madison, WI) or standard diet without supplementation ad libitum for up to 12 wk. All rats were provided free access to tap water and a salt block to maintain sodium balance and prevent acute lithium intoxication. Rats were individually housed in single rat metabolic cages for a 24-h acclimation period followed by an additional 24 h to collect urine under oil for analysis.

Analysis of urine and serum samples. Urine pH was measured by Corning pH Meter 440. Urine osmolality was measured on a Wescor 5520 Vapor Pressure Osmometer (Wescore, Logan, UT). Urinary and serum sodium, chloride, and potassium, as well as serum lithium, were measured by EasyLyte instrument and normalized to urinary creatinine as determined by the Jaffe reaction. Urinary ammonium was measured using an ammonia detection kit produced by Pointe Scientific, used according to manufacturer specifications, and normalized to urinary creatinine. In all tests, control, $n = 11$; 1 wk, $n = 7$; 2 wk, $n = 6$; 3 wk, $n = 8$; 6 wk, $n = 10$; 9 wk, $n = 3$; 12 wk, $n = 3$.

Immunofluorescence. Tissues were prepared as previously described (5). Whole kidney sections were hydrated with ethanol, and endogenous peroxides were quenched with 3% H_2O_2. Antigen retrieval was accomplished using Tris-EGTA-buffer (TEG; 10 mM Tris, 0.5 mM EGTA, pH 9.0), and free aldehyde groups were quenched with 50 mM NH_4Cl-PBS. Sections were then blocked in 1% BSA-PBS for 30 min at room temperature. Sections were incubated overnight at 4°C with an antibody specific to AQP4 (1:200, sc-20812; Santa Cruz Biotechnology), V-ATPase B1/2 (1:300, sc-55544; Santa Cruz Biotechnology), pendrin (1:1,000, provided by Dr. Susan Wall), or PCNA (1:50, sc-9857; Santa Cruz Biotechnology). After several PBS washes, sections were incubated for 2 h at room temperature with an Alexa Fluor® 546 or Alexa Fluor® 488 secondary (Invitrogen) specific to the appropriate primary host species (Invitrogen). Sections intended for TUNEL analysis were treated with an In Situ Cell Death Detection Kit (Roche Diagnostics, Mannheim, Germany). After three PBS washes, sections were mounted with ProLong Gold Antifade with DAPI (Cell Signaling, Danvers, MA).

Fluorescent images were recorded under an Olympus IX71 inverted microscope and analyzed using the functionally equivalent "multipointer" or "cell counter" plugins in ImageJ; $n = 3$ unless otherwise noted.

Statistical analyses. Proportional data are expressed as means ± SE of the proportion; these data were arcsine transformed before statistical analysis. All other data are expressed as means ± SE. Differences were determined by Kruskal-Wallis one-way ANOVA and Tukey's post hoc test. Throughout, asterisks indicate a significant difference from control. All calculations were performed using GraphPad Prism 7.0 software (GraphPad Software, La Jolla, CA).

RESULTS

Severity of lithium-induced polyuria is constant from 2 to 12 wk of lithium treatment. To monitor the extent of lithium-induced polyuria over long-term treatment regimens, rats were fed either a standard diet or a lithium-containing diet for 1, 2, 3, 6, 9, or 12 wk. After 1 wk of lithium treatment, serum lithium levels were significantly higher than serum lithium levels in untreated animals (Fig. 1*A*). Serum lithium levels

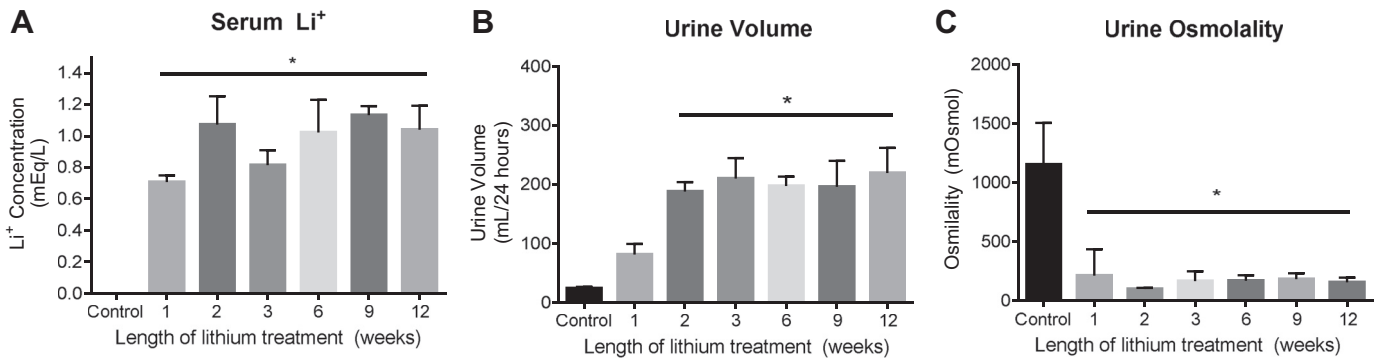

Fig. 1. Physiological analyses of lithium-induced polyuria over 12 wk of lithium treatment. Male rats were fed a 40 mmol/kg lithium diet for 0, 1, 2, 3, 6, 9, or 12 wk. Single animals were subsequently placed in individual metabolic cages to collect urine and serum at the determined time point. *A*: serum lithium levels were measured using an EasyLyte according to the manufacturer's instructions. *B*: urine was collected over 24 h under oil to prevent evaporation. *C*: urine osmolality was measured from collected urine. Data are presented as means ± SE, where $*P < 0.05$ vs. control. Control, $n = 11$; 1 wk, $n = 7$; 2 wk, $n = 6$; 3 wk, $n = 8$; 6 wk, $n = 10$; 9 wk, $n = 3$; 12 wk, $n = 3$.

Table 1. *Urine and serum ion concentrations*

Length of Lithium Treatment	Sodium		Chloride		Potassium	
	Urine, meq/mg	Serum, meq/l	Urine, meq/mg	Serum, meq/l	Urine, meq/mg	Serum, meq/l
Control	1.807 ± 1.178	139.5 ± 0.481	2.780 ± 0.269	102.7 ± 1.858	3.855 ± 0.331	5.493 ± 0.961
1 Week	1.681 ± 0.224	139.4 ± 0.971	2.502 ± 0.521	107.8 ± 0.752	2.493 ± 0.273	5.938 ± 0.582
2 Weeks	2.659 ± 0.696	132.2 ± 8.582	6.763 ± 1.905	105.7 ± 6.756	5.206 ± 1.447	6.097 ± 0.707
3 Weeks	3.277 ± 0.650	137.5 ± 1.391	3.448 ± 0.616	107.0 ± 0.338	4.004 ± 1.113	8.077 ± 1.172
6 Weeks	4.836 ± 0.953*	149.1 ± 4.661	5.138 ± 1.351	113.8 ± 5.607	6.420 ± 1.606	4.857 ± 0.049
9 Weeks	6.386 ± 1.269*	139.0 ± 1.822	3.401 ± 1.268	110.1 ± 1.457	6.390 ± 2.316	9.180 ± 0.042
12 Weeks	3.354 ± 0.249	148.3 ± 3.300	2.401 ± 0.076	114.7 ± 3.300	5.112 ± 1.682	7.680 ± 0.176

Data are expressed as means ± SE and subjected to a Kruskal-Wallis one-way ANOVA and Tukey's post hoc test. Serum sodium, chloride, and potassium were measured by EasyLyte. Urinary sodium, chloride, and potassium levels were also measured by EasyLyte and normalized to urinary creatinine to compensate for varying urine volume. Concentrations are presented as normalized to urinary creatinine. Control, $n = 11$; 1 wk, $n = 7$; 2 wk, $n = 6$; 3 wk, $n = 8$; 6 wk, $n = 10$; 9 wk, $n = 3$; 12 wk, $n = 3$. *$P < 0.05$ vs. control.

remained elevated in rats treated for 2, 3, 6, 9, and 12 wk. Furthermore, serum lithium levels were not significantly different among treatment periods, and, in all groups, serum lithium concentrations were comparable to therapeutic levels in humans (0.8–1.3 meq/l) (16). Although 24-h urine output was elevated in rats treated with lithium for 1 wk compared with untreated rats, urine volume was not significantly different between the two groups of animals. Rats treated with lithium for 2, 3, 6, 9, and 12 wk had a significantly higher 24-h urine output than untreated- and 1-wk-treated rats, but the volumes were not significantly different from each other (Fig. 1*B*). In addition to the increase in 24-h urine output, lithium-fed rats also displayed a significantly lower urine osmolality after 1, 2, 3, 6, 9, and 12 wk of lithium treatment compared with untreated animals (Fig. 1*C*). In sum, rats treated with lithium from 2 through 12 wk of treatment produced ~10 times as much urine as untreated rats, and said urine was roughly 10 times as dilute as that of untreated rats, corroborating the establishment of polyuria with lithium treatment.

Serum sodium, chloride, and potassium concentrations were monitored for each treatment group, and no significant differences were observed (Table 1). Sodium, chloride, and potassium were also measured in urine collected from each treatment group. Rats treated with lithium for 6 and 9 wk had a slightly significant increase in urinary sodium levels (Table 1). Otherwise, no significant differences in urinary sodium, chloride, and potassium levels were observed in the treated rats.

Substantial cell proliferation occurs at 1 and 2 wk of lithium treatment. Lithium treatment is known to cause IMCD remodeling (9, 12, 34, 37); however, studies in rodents have not exceeded 4 wk in previous reports. To examine the effect on long-term lithium treatment on cellular proliferation in the IMCD, we assessed the expression of PCNA in kidney sections from rats treated with lithium for 0, 1, 2, 3, 6, 9, and 12 wk. Immunofluorescence staining of rat kidney sections revealed extensive labeling of PCNA in the principal cells at 1 wk (Fig. 2*B*) and 2 wk (Fig. 2*C*) of lithium treatment compared with untreated animals (Fig. 2*A*). Compared with untreated rats,

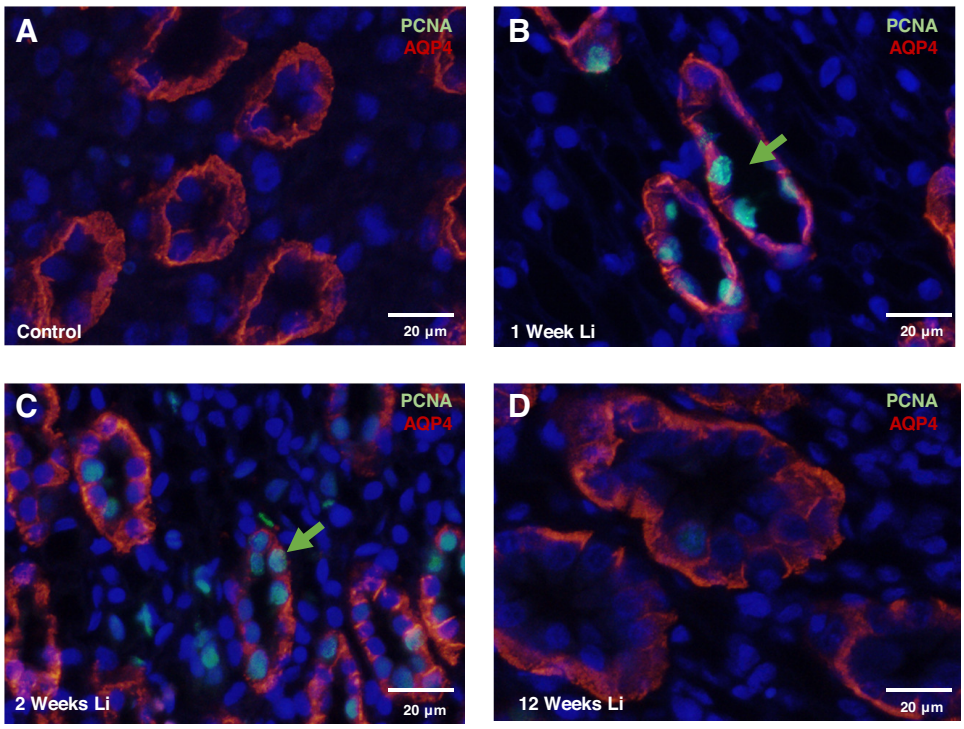

Fig. 2. Inner medullary collecting duct (IMCD) principal cells label positively for proliferating cell nuclear antigen (PCNA) during early lithium treatment. Shown are representative images from kidney inner medullary tissue (IM-3) stained for the proliferation marker PCNA (green) and the renal principal cell marker, aquaporin-4 (AQP4) (red) in untreated rats (*A*), 1-wk lithium-treated rats (*B*), 2-wk lithium-treated rats (*C*), and 12-wk lithium-treated rats (*D*). Nuclei are stained blue with DAPI; $n = 3$.

there was no significant PCNA staining in the principal cells of rats treated for 3, 6, 9, and 12 wk (data not shown and Fig. 2*D*). It is possible that principal cell proliferation appeared to cease in 3- to 12-wk lithium-treated rats due to an increase in principal cell apoptosis; however, TUNEL analysis did not yield any evidence of significant apoptosis at any given time interval of lithium treatment (data not shown and Fig. 3, *A–D*).

It is important to note that PCNA is expressed during the S-phase of the cell cycle, and it has been suggested that a number of these cells may be arrested in the G2 phase (10). Our findings appear to be consistent with previous published work.

Lithium induces sustained IMCD remodeling starting at 2 wk of lithium treatment. Previous studies demonstrate that another effect of lithium treatment is an increase in the number of intercalated cells compared with principal cells in the IM-1 and IM-2 regions of the IMCD (8). Immunofluorescence labeling for AQP4 (a basolateral principal cell marker) and V-ATPase (an intercalated cell marker) of kidney sections (IM-1 and IM-2) was performed in rats treated with lithium for 0, 1, 2, 3, 6, 9, and 12 wk. The fraction of principal cells to intercalated cells was determined using these markers (Fig. 4*H*). This double labeling demonstrated the expected trend of early-stage remodeling in the IMCD (8, 10, 21, 34). In untreated rats (Fig. 4*A*), rats treated for 1 wk (Fig. 4*B*), rats treated for 2 wk (Fig. 4*C*), and rats treated for 3 wk (Fig. 4*D*), ~90% of cells in the initial inner medulla (IM-1 and IM-2) label only for AQP4. The remaining cells chiefly label for V-ATPase, and are presumably A-type intercalated cells.

At 6 wk of lithium treatment, the fraction of V-ATPase-positive cells to AQP4-positive cells in the rat IM-1 and IM-2 sections increased significantly (Fig. 4*E*): roughly 25% of cells were V-ATPase positive (Table 2). This trend continued into the 9-wk treatment group (Fig. 4*F*), where roughly 43% of cells were V-ATPase positive (Table 2). There was no further shift to the cellular fraction from 9 to 12 wk of treatment (Fig. 4*G*).

Lithium induces various atypical expression and localization patterns of intercalated cell types. Thus far, few studies have examined the effect of lithium on intercalated cell type in the inner medulla. As previously discussed, intercalated cells in the IM are generally A-type, while those found in the cortex are A-type, B-type, and non-A non-B type; these latter two cell types express pendrin (23, 47, 48).

Immunofluorescence labeling for V-ATPase and pendrin of kidney IM sections was performed in rats treated with lithium for 0, 1, 2, 3, 6, 9, and 12 wk to characterize the intercalated cell types that make up the increased number of intercalated cells in this region of the kidney. Unexpectedly, from 6 to 12 wk of lithium treatment, immunofluorescence labeling revealed pendrin expression in rat IM-3 (Fig. 5, *A–C*). As previously mentioned, pendrin-expressing intercalated cells are generally found in the distal convoluted tubule, the cortical collecting duct, and the connecting tubule; A-type intercalated cells can be found up to the initial portion of the IMCD (47). In a coronal section, this means that intercalated cells become increasingly rare, and ultimately absent, as one descends from the initial IM toward the papillary tip. From 6 to 12 wk of lithium treatment, all observed intercalated cell types were detected in every portion of the IM, including the inner medullary tip (Fig. 5, *D* and *E*).

Immunofluorescent labeling of V-ATPase revealed that both known pendrin-expressing intercalated cell phenotypes were present in the IM (Fig. 6, *A–C*). Interestingly, 1–10% of cells expressed pendrin and not V-ATPase, a phenotype not previously reported. When we concurrently tagged pendrin and AQP4 (a principal cell marker), we recorded coincident expression at the same frequency, qualitatively (Fig. 6*D*).

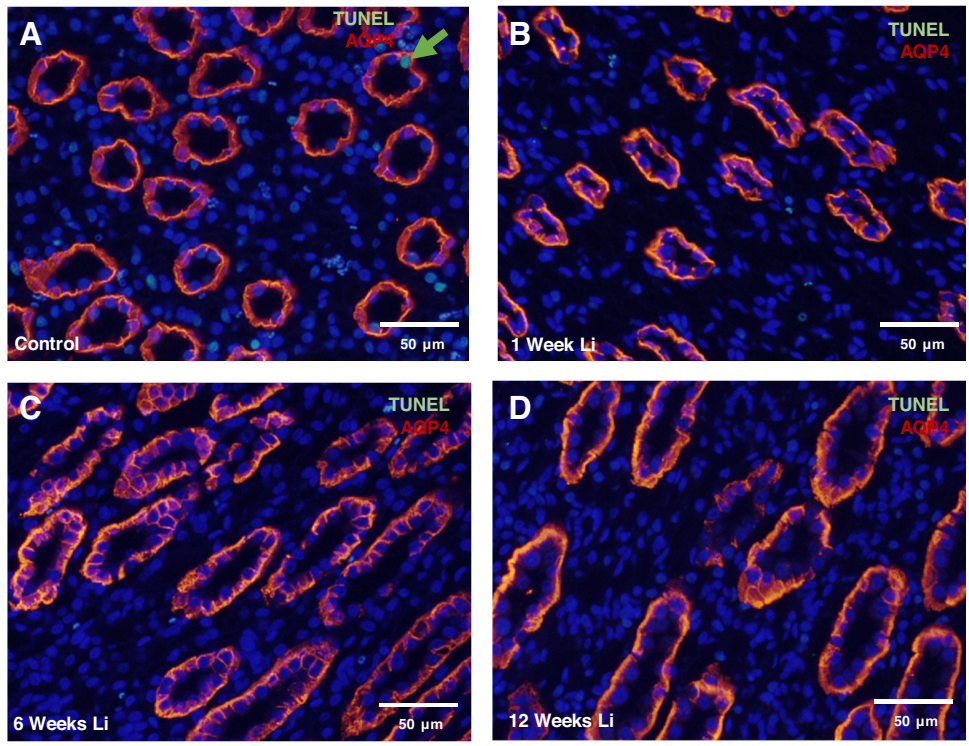

Fig. 3. Inner medullary collecting duct (IMCD) principal cells are not apoptotic during lithium treatment. Shown are representative images from kidney IM-3 tissue stained for the renal principal cell marker aquaporin-4 (AQP4) (red) following a TUNEL assay (green) in untreated rats (*A*), 1-wk lithium-treated rats (*B*), 6-wk lithium-treated rats (*C*), and 12-wk lithium-treated rats (*D*). Nuclei are stained blue with DAPI; $n = 3$.

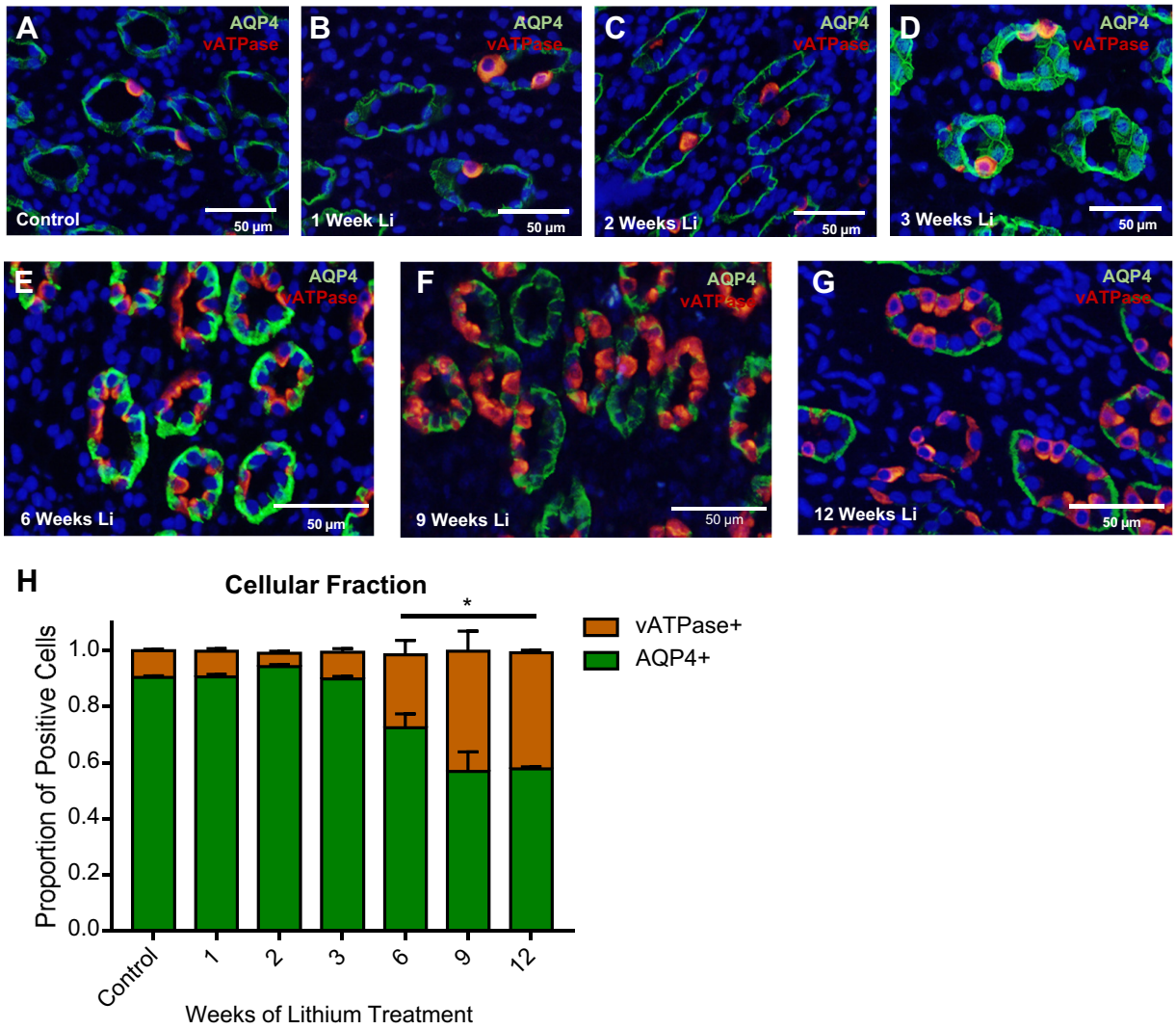

Fig. 4. Chronic lithium treatment induces inner medullary collecting duct (IMCD) remodeling. Shown are representative images from kidney inner medullary (IM) tissue stained for the renal principal cell marker aquaporin-4 (AQP4) (green) and an intercalated cell marker vacuolar H^+-ATPase (V-ATPase; red), in untreated rats (*A*), 1-wk lithium-treated rats (*B*), 2-wk lithium-treated rats (*C*), 3-wk lithium-treated rats (*D*), 6-wk lithium-treated rats (*E*), 9-wk lithium-treated rats (*F*), and 12-wk lithium-treated rats (*G*). *H*: quantification of the proportions of AQP4-positive and V-ATPase-positive cells. Data are presented as mean proportion ± SE of the proportion, where $*P < 0.05$ vs. control. For figure clarity, cells both AQP4 and V-ATPase positive were excluded from this analysis, but their proportion can be found in Table 2. Nuclei are stained blue with DAPI; $n = 3$.

Early lithium-mediated increases in urinary pH and NH_4^+ are ameliorated with longer treatment. Because intercalated cells play a role in acid-base homeostasis (38), we suspected that changes in the phenotypic profile of intercalated cells might affect acid-base concentrations in the urine. At 1 wk of lithium treatment, urine pH was significantly increased (Fig. 7*A*). Urine pH then decreased to baseline (or modestly below baseline, although the differences were not statistically significant). Urinary pH qualitatively stabilizes between 3 and 12 wk of treatment.

To buffer endogenous and exogenous acid loads, renal tissue must maintain a store of HCO_3^-; this is accomplished via ammoniagenesis, which generates an equal proportion of NH_4^+ and HCO_3^- (50). Furthermore, NH_4^+ excretion is one of the primary mechanisms used by the renal system in response to metabolic acidosis (50). Measures of urinary NH_4^+ would therefore tell us a great deal about how acid-base homeostasis shifts in response to shifts in blood and urinary pH. Urinary NH_4^+ appears to trend upward at 1 wk of treatment, and this increase is statistically significant at 2 wk (Fig. 7*B*). Much like pH, ammonium levels decrease to baseline and are stabilized between 3 and 12 wk of treatment.

DISCUSSION

Differences in early- and late-stage lithium-induced collecting duct remodeling. It has been previously described that lithium treatment induces an increase in the fraction of intercalated cells in the renal collecting duct (9, 10, 12, 21, 34, 44). The patterns of proliferation, apoptosis, and A-type intercalated cell remodeling that we observed were in line with these previous studies.

Our observations reveal, however, that late-stage remodeling includes aberrant patterns of pendrin and V-ATPase expression along the collecting duct. Pendrin is normally expressed in the

Table 2. *Breakout of CD architecture*

Length of Lithium Treatment	Percent, %			Cells/CD Section
	AQP4$^+$ V-ATPase$^-$	AQP4$^-$ V-ATPase$^+$	AQP4$^+$ V-ATPase$^+$	
Control	90.5 ± 0.565	9.50 ± 0.565	0.00 ± 0.00	6.05 ± 0.976
1 Week	90.7 ± 0.875	9.22 ± 0.871	0.0895 ± 0.0584	7.40 ± 0.700
2 Weeks	94.3 ± 0.744	4.91 ± 0.609	0.836 ± 0.177	7.07 ± 0.936
3 Weeks	89.9 ± 0.969	9.59 ± 1.31	0.513 ± 0.416	9.22 ± 0.936
6 Weeks	72.6 ± 4.89*	26.1 ± 5.09*	1.39 ± 0.275	9.04 ± 1.99
9 Weeks	56.8 ± 7.02*	43.1 ± 7.03*	0.108 ± 0.0560	8.74 ± 1.15
12 Weeks	57.8 ± 0.829*	41.4 ± 1.06*	0.829 ± 0.352	10.2 ± 1.30

Data are presented as percentages or number of cells per collecting duct and are expressed as mean proportion ± SE of the proportion. CD, collecting duct. With the use of mages collected from the terminal inner medullary (IM) region, cells that expressed only aquaporin-4 (AQP4), only vacuolar H^+-ATPase (V-ATPase), or both AQP4 and V-ATPase were analyzed using the functionally equivalent "multipointer" or "cell counter" plugins in ImageJ software. Arcsine-transformed data were subjected to a Kruskal-Wallis one-way ANOVA and Tukey's post hoc test. *$P < 0.05$ vs. control; $n = 3$ wk.

distal convoluted tubule, the cortical collecting duct, and the connecting tubule (38, 47). V-ATPase is found in many areas along the nephron but is normally absent in the terminal portions of the collecting duct. After lithium treatment, however, we observed pendrin and V-ATPase expression throughout the IM, including the terminal portions.

The current model, whereby PCNA-positive principal cells are arrested in the G2 phase of the cell cycle, allowing intercalated cells to outpace them in cell division (10), seems to reasonably account for some aspects of IMCD remodeling. However, this model does not account for these late-stage changes to intercalated cell-associated protein expression. Mechanisms other than proliferation must be involved in these novel patterns of pendrin and V-ATPase expression, and localization, in the IMCD.

Plasticity as a contributor to collecting duct remodeling. Although the way by which intercalated and principal cells differentiate is not totally clear, there is some substantial evidence that renal cells, intercalated cells in particular, are plastic into maturity (29). Intercalated cells are known to change their phenotype in response to upsets in acid-base homeostasis (1). It has been suggested that non-A, non-B intercalated cells are an intermediate step in intercalated cell conversion in response to these upsets (20, 42). Intercalated cells have been shown in vitro as being capable of differentiating into principal cells (13). Furthermore, cells colabeled for principal and intercalated cell markers have been previously observed during lithium recovery and were suggested to be intercalated cells converting back to principal cells (44).

Given the lack of proliferation or apoptosis associated with continued fractional changes to IMCD cells, the presence of

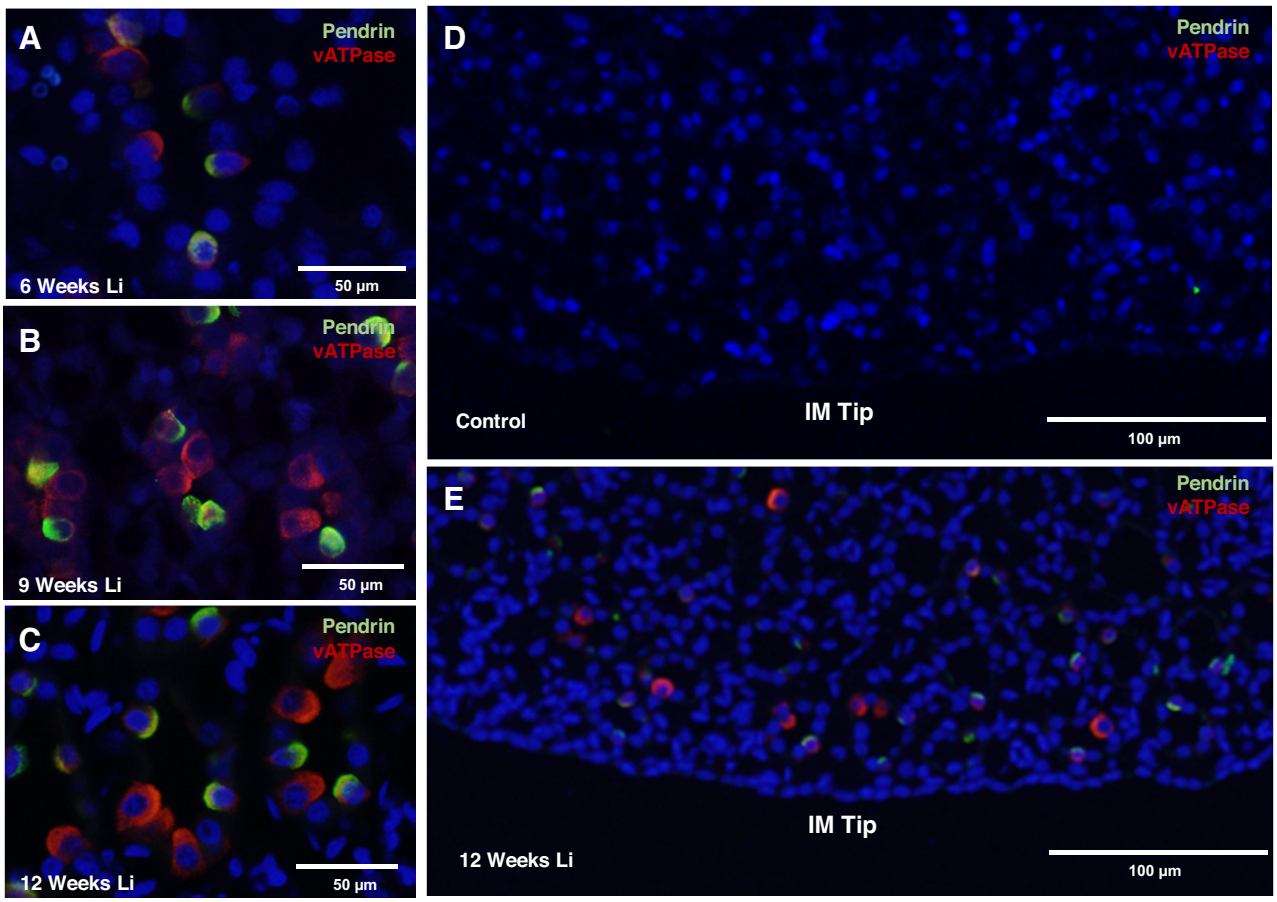

Fig. 5. Chronic lithium treatment induces aberrant patterns of intercalated cell type expression in the kidney. Shown are representative images from kidney inner medullary (IM) tissue stained for an intercalated cell marker and vacuolar H^+-ATPase (V-ATPase) (red) and pendrin (green) in 6-wk lithium-treated rats (*A*), 9-wk lithium-treated rats (*B*), and 12-wk lithium-treated rats (*C*). *D* and *E*: representative images at a lower magnification of staining in untreated and 12-wk lithium-treated rats. Nuclei are stained blue with DAPI; $n = 3$.

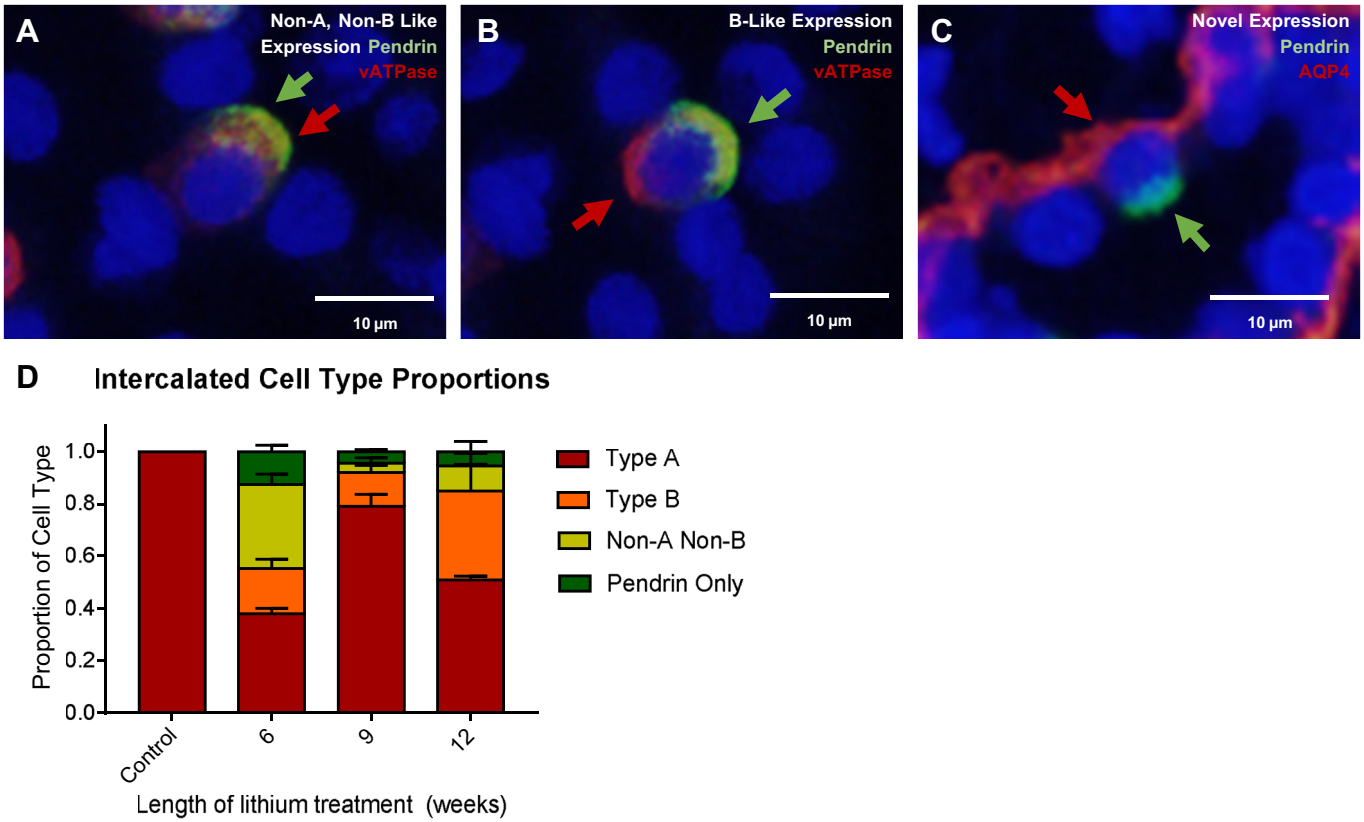

Fig. 6. Altered intercalated cell types are observed after chronic lithium treatment. Shown are representative images from kidney inner medullary (IM) tissue from 12-wk lithium-treated rats stained for an intercalated cell marker vacuolar H^+-ATPase (V-ATPase) (red) and pendrin (green). Observed were the following cell types: non-A, non-B type intercalated cells (*A*); B-type intercalated cells (*B*), and a novel renal cell phenotype (*C*), wherein both pendrin and aquaporin-4 (AQP4) (red), a principal cell marker, are expressed. *D*: quantification proportions of different intercalated cell types. Control, $n = 3$; 6 wk, $n = 2$, 9 wk, $n = 3$, 12 wk, $n = 2$.

cells labeled for both intercalated and principal cell markers, and the presence of intercalated cell markers where there are normally only principal and/or IMCD cells, our data collectively suggest that renal cell plasticity, in particular, principal-to-intercalated cell conversion, is in some way responsible for lithium-induced, late-stage changes to collecting duct morphology.

Acid-base homeostasis and modifications to intercalated cells. Hyperchloremic metabolic acidosis has been reported in rats undergoing lithium treatment (21). We observed a significant increase in urine pH at 3 wk of treatment and a subsequent increase in the number of V-ATPase-positive cells. Although we did not independently evidence metabolic acidosis in our study, these observations are largely consistent with previous suggestions that V-ATPase expression may be upregulated as a compensatory response to systemic metabolic acidosis (21).

Changes to acid-base homeostasis have also been suggested to affect pendrin expression (24). Counterintuitively, urinary pH and urinary ammonium levels were not significantly altered in animals showing aberrant patterns of pendrin and V-ATPase expression despite being altered during the early stages of lithium treatment. Previous studies had indicated that urine pH is decreased in rats following 4 wk of lithium treatment, and it has been subsequently suggested that changes in V-ATPase expression constitute a compensatory response to distal renal

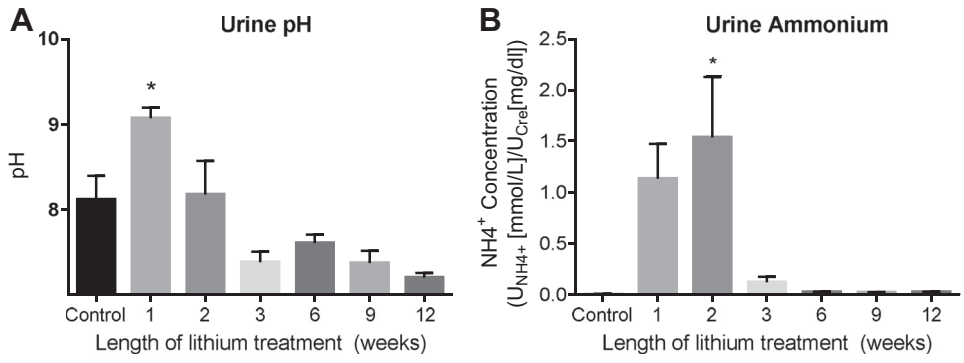

Fig. 7. Acid-base homeostasis was disrupted during lithium treatment. *A*: urine pH was measured in urine collected under oil from rats in fed a 40 mmol/kg lithium diet for 0, 1, 2, 3, 6, 9, or 12 wk. *B*: urine ammonium was measured according to manufacturer's instructions in urine collected under oil from rats fed a 40 mmol/kg lithium diet for 0, 1, 2, 3, 6, 9, or 12 wk. Data are presented as means ± SE, where $*P < 0.05$ vs. control. Control, $n = 11$; 1 wk, $n = 7$; 2 wk, $n = 6$; 3 wk, $n = 8$; 6 wk, $n = 10$; 9 wk, $n = 3$; 12 wk, $n = 3$.

tubular acidosis (21). From 3 to 12 wk of treatment, although the differences in pH were not significant, the means were markedly lower (Fig. 7*B*). With previous studies in mind, we suspect it may be the case that differences in pH were masked by our relatively small sample size.

Previous studies are consistent with our own, in that pendrin expression remained unchanged up to 4 wk of lithium treatment (21). The expression of pendrin, however, has been previously suggested to change in response to upsets in acid-base homeostasis (14). If V-ATPase expression is upregulated in response to lithium-induced upsets to acid-base homeostasis, but these expression level changes are not tightly controlled, it may be the case that the changes in pendrin expression (and by extension, an increase of the fraction of pendrin-expressing cells) that we observed occur in response to overcompensation by the drastically increased population of A-type intercalated cells.

However, the exact mechanisms by which renal epithelial cells sense and respond to acidosis are unclear. Several studies have implicated endothelin receptor activation in pH sensing. Acidosis induces endothelin synthesis in renal epithelia, increases endothelin concentrations in the interstitium, and increases endothelin-1 mRNA abundance in the renal cortex (1, 51, 52). Endothelin expression is, in fact, vital to this process, as endothelin B (ETB) inhibition inhibits the ability of the distal nephron to respond to acidosis (1). Tyrosine kinases probably play some role in this mechanism; ETB activation is known to increase tyrosine phosphorylation of proximal tubule cells, and acidosis is associated with increases in the activity of c-src and focal adhesion kinase, two tyrosine kinases (27, 53).

Intracellular acidosis has also been correlated with increases in the intracellular calcium concentrations that mediate apical vesicle fusion (6, 45). This does not appear to be necessary to pH-induced plasticity as buffering calcium concentrations does not prevent B- to A-type conversion (39).

More direct studies are needed to elucidate the exact relationship between lithium-induced changes in pendrin localization and lithium-induced aberrations to renal acid-base homeostasis.

Roles of epithelial architecture and luminal constituents in modifications to intercalated cells. Epithelial architecture, specifically, the density of the extracellular matrix, can affect the polarity of intercalated cells; plating of cells in high density switches the polarity of H^+-ATPase and AE1 from apical to basolateral and vice-versa, respectively (46). The protein hensin is thought to play a role in this process, as injection of hensin protein into the extracellular matrix is sufficient for inducing polarity switching (41, 46). This sort of plasticity is known to occur during development; Na^+-K^+-ATPase is expressed apically in mammalian embryos but is increasingly basolateral in its expression pattern as the tissue matures (3).

As previously discussed, renal principal cells may be arrested in the G2 phase, and it has been suggested that this may contribute to renal tubular fibrosis (10). We noticed a trend of an increased number of cells per collecting duct as treatment progressed, but these differences were not statistically different (Table 2). More directed studies are required to determine whether and how lithium-induced fibrosis might contribute to the sort of cell-type switching we have observed.

Changes in luminal flow, luminal solute concentration, and other epithelial properties, modulate pendrin expression (24). Lithium-induced polyuria was observed in these animals, suggesting that increased luminal flow might play some causal role in increases to pendrin expression. Urine volumes reached maximum at 2 wk of treatment and were maintained at that level for the length of the study. Because pendrin did not appear in the IM until 6 wk of treatment, it does not appear that these changes in luminal flow are sufficient for inducing the observed patterns of pendrin expression. It also does not explain how pendrin might have come to be expressed in areas where it is normally absent.

Lithium treatment has been previously associated with hypernatremia and, in at least one case study, hyperkalemia (15, 28). However, we did not detect any significant changes to serum sodium or potassium ion concentration during our study. It is worth taking into consideration the low sample size (n = 3) of our 9- and 12-wk treatment groups; a larger sample size might have elucidated some difference. As such, the role that luminal solute concentration might play is not clear.

Importance of renal remodeling to lithium-induced nephropathies. The changes in pendrin and V-ATPase expression that we observed are in some ways not surprising; we know of many mechanisms that can drive phenotype switching. Changes to protein localization in the nephron, however, are surprising and interesting. These observations add to collective evidence that renal epithelial cells maintain an incredible amount of phenotypic plasticity into maturity. Understanding the mechanisms of this plasticity is important for understanding the cellular mechanisms of lithium-induced disease, but it might also shed some light on epithelial development in general. As previously noted, some amount of plasticity occurs following cessation of lithium treatment. Specifically, it has been suggested that intercalated cells convert to principal cells, presumably undoing changes to IMCD induced by the lithium treatment itself (44). Continued work in this area will hopefully reveal some targetable cellular mechanisms by which we can reverse the damage done by lithium and other nephrotoxic drugs.

ACKNOWLEDGMENTS

We thank Dr. David Weiner, Gunar Osis, and Dr. Derek Pham for technical assistance. We also thank Dr. Susan Wall for providing us with pendrin antibody.

GRANTS

This study was funded by a Norman S. Coplon Extramural Grant granted from Satellite Healthcare to M. A. Blount in addition to internal funding support from Emory University School of Medicine to M. A. Blount. D. A. Rodriguez was supported by a Scholarly Inquiry and Research at Emory Fellowship, Y. Wang was supported by Howard Hughes Medical Institute (HHMI) Award 52006923, and M. A. Sun was supported by the National Institutes of Health (NIH) - National Institute of Diabetes and Digestive and Kidney Diseases Grant R25-DK-101390.

DISCLOSURES

No conflicts of interest, financial or otherwise, are declared by the authors.

AUTHOR CONTRIBUTIONS

N.J.H. and M.A.B. conceived and designed research; N.J.H., Y.W., D.A.R., M.A.S., and M.A.B. performed experiments; N.J.H., Y.W., D.A.R., M.A.S., and M.A.B. analyzed data; N.J.H. and M.A.B. interpreted results of experiments; N.J.H. and M.A.B. prepared figures; N.J.H. and M.A.B. drafted manuscript; N.J.H. and M.A.B. edited and revised manuscript; N.J.H., Y.W., D.A.R., M.A.S., and M.A.B. approved final version of manuscript.

REFERENCES

1. **Al-Awqati Q.** Terminal differentiation of intercalated cells: the role of hensin. *Annu Rev Physiol* 65: 567–583, 2003. doi:10.1146/annurev.physiol.65.092101.142645.
2. **Alper SL, Natale J, Gluck S, Lodish HF, Brown D.** Subtypes of intercalated cells in rat kidney collecting duct defined by antibodies against erythroid band 3 and renal vacuolar H+-ATPase. *Proc Natl Acad Sci USA* 86: 5429–5433, 1989. doi:10.1073/pnas.86.14.5429.
3. **Avner ED, Sweeney WE Jr, Nelson WJ.** Abnormal sodium pump distribution during renal tubulogenesis in congenital murine polycystic kidney disease. *Proc Natl Acad Sci USA* 89: 7447–7451, 1992. doi:10.1073/pnas.89.16.7447.
4. **Blount MA, Mistry AC, Fröhlich O, Price SR, Chen G, Sands JM, Klein JD.** Phosphorylation of UT-A1 urea transporter at serines 486 and 499 is important for vasopressin-regulated activity and membrane accumulation. *Am J Physiol Renal Physiol* 295: F295–F299, 2008. doi:10.1152/ajprenal.00102.2008.
5. **Blount MA, Sim JH, Zhou R, Martin CF, Lu W, Sands JM, Klein JD.** Expression of transporters involved in urine concentration recovers differently after cessation of lithium treatment. *Am J Physiol Renal Physiol* 298: F601–F608, 2010. doi:10.1152/ajprenal.00424.2009.
6. **Cannon C, van Adelsberg J, Kelly S, Al-Awqati Q.** Carbon-dioxide-induced exocytotic insertion of H+ pumps in turtle-bladder luminal membrane: role of cell pH and calcium. *Nature* 314: 443–446, 1985. doi:10.1038/314443a0.
7. **Chiu C-T, Wang Z, Hunsberger JG, Chuang D-M.** Therapeutic potential of mood stabilizers lithium and valproic acid: beyond bipolar disorder. *Pharmacol Rev* 65: 105–142, 2013. doi:10.1124/pr.111.005512.
8. **Christensen BM, Kim Y-H, Kwon T-H, Nielsen S.** Lithium treatment induces a marked proliferation of primarily principal cells in rat kidney inner medullary collecting duct. *Am J Physiol Renal Physiol* 291: F39–F48, 2006. doi:10.1152/ajprenal.00383.2005.
9. **Christensen BM, Marples D, Kim Y-H, Wang W, Frøkiaer J, Nielsen S.** Changes in cellular composition of kidney collecting duct cells in rats with lithium-induced NDI. *Am J Physiol Cell Physiol* 286: C952–C964, 2004. doi:10.1152/ajpcell.00266.2003.
10. **de Groot T, Alsady M, Jaklofsky M, Otte-Höller I, Baumgarten R, Giles RH, Deen PMT.** Lithium causes G2 arrest of renal principal cells. *J Am Soc Nephrol* 25: 501–510, 2014. doi:10.1681/ASN.2013090988.
11. **de Groot T, Sinke AP, Kortenoeven MLA, Alsady M, Baumgarten R, Devuyst O, Loffing J, Wetzels JF, Deen PMT.** Acetazolamide attenuates lithium-induced nephrogenic diabetes insipidus. *J Am Soc Nephrol* 27: 2082–2091, 2016. doi:10.1681/ASN.2015070796.
12. **Ecelbarger CA.** Lithium treatment and remodeling of the collecting duct. *Am J Physiol Renal Physiol* 291: F37–F38, 2006. doi:10.1152/ajprenal.00046.2006.
13. **Fejes-Tóth G, Náray-Fejes-Tóth A.** Differentiation of renal beta-intercalated cells to alpha-intercalated and principal cells in culture. *Proc Natl Acad Sci USA* 89: 5487–5491, 1992. doi:10.1073/pnas.89.12.5487.
14. **Frische S, Kwon T-H, Frøkiaer J, Madsen KM, Nielsen S.** Regulated expression of pendrin in rat kidney in response to chronic NH_4Cl or $NaHCO_3$ loading. *Am J Physiol Renal Physiol* 284: F584–F593, 2003. doi:10.1152/ajprenal.00254.2002.
15. **Goggans FC.** Acute hyperkalemia during lithium treatment of manic illness. *Am J Psychiatry* 137: 860–861, 1980. doi:10.1176/ajp.137.7.860.
16. **Grandjean EM, Aubry JM.** Lithium: updated human knowledge using an evidence-based approach. Part II: Clinical pharmacology and therapeutic monitoring. *CNS Drugs* 23: 331–349, 2009. doi:10.2165/00023210-200923040-00005.
17. **Grünfeld J-P, Rossier BC.** Lithium nephrotoxicity revisited. *Nat Rev Nephrol* 5: 270–276, 2009. doi:10.1038/nrneph.2009.43.
18. **Hoffert JD, Pisitkun T, Wang G, Shen R-F, Knepper MA.** Quantitative phosphoproteomics of vasopressin-sensitive renal cells: regulation of aquaporin-2 phosphorylation at two sites. *Proc Natl Acad Sci USA* 103: 7159–7164, 2006. doi:10.1073/pnas.0600895103.
19. **Kamsteeg E-J, Hendriks G, Boone M, Konings IBM, Oorschot V, van der Sluijs P, Klumperman J, Deen PMT.** Short-chain ubiquitination mediates the regulated endocytosis of the aquaporin-2 water channel. *Proc Natl Acad Sci USA* 103: 18344–18349, 2006. doi:10.1073/pnas.0604073103.
20. **Kim J, Kim Y-H, Cha J-H, Tisher CC, Madsen KM.** Intercalated cell subtypes in connecting tubule and cortical collecting duct of rat and mouse. *J Am Soc Nephrol* 10: 1–12, 1999.
21. **Kim Y-H, Kwon T-H, Christensen BM, Nielsen J, Wall SM, Madsen KM, Frøkiaer J, Nielsen S.** Altered expression of renal acid-base transporters in rats with lithium-induced NDI. *Am J Physiol Renal Physiol* 285: F1244–F1257, 2003. doi:10.1152/ajprenal.00176.2003.
23. **Kim Y-H, Kwon T-H, Frische S, Kim J, Tisher CC, Madsen KM, Nielsen S.** Immunocytochemical localization of pendrin in intercalated cell subtypes in rat and mouse kidney. *Am J Physiol Renal Physiol* 283: F744–F754, 2002. doi:10.1152/ajprenal.00037.2002.
24. **Kim YH, Pham TD, Zheng W, Hong S, Baylis C, Pech V, Beierwaltes WH, Farley DB, Braverman LE, Verlander JW, Wall SM.** Role of pendrin in iodide balance: going with the flow. *Am J Physiol Renal Physiol* 297: F1069–F1079, 2009. doi:10.1152/ajprenal.90581.2008.
25. **Kishore BK, Ecelbarger CM.** Lithium: a versatile tool for understanding renal physiology. *Am J Physiol Renal Physiol* 304: F1139–F1149, 2013. doi:10.1152/ajprenal.00718.2012.
26. **Klein JD, Blount MA, Sands JM.** Molecular mechanisms of urea transport in health and disease. *Pflugers Arch* 464: 561–572, 2012. doi:10.1007/s00424-012-1157-0.
27. **Laghmani K, Preisig PA, Moe OW, Yanagisawa M, Alpern RJ.** Endothelin-1/endothelin-B receptor-mediated increases in NHE3 activity in chronic metabolic acidosis. *J Clin Invest* 107: 1563–1569, 2001. doi:10.1172/JCI11234.
28. **Liamis G, Milionis HJ, Elisaf M.** A review of drug-induced hypernatraemia. *NDT Plus* 2: 339–346, 2009.
29. **Little M, Georgas K, Pennisi D, Wilkinson L.** Kidney development: two tales of tubulogenesis. *Curr Top Dev Biol* 90: 193–229, 2010. doi:10.1016/S0070-2153(10)90005-7.
30. **Mann L, Heldman E, Shaltiel G, Belmaker RH, Agam G.** Lithium preferentially inhibits adenylyl cyclase V and VII isoforms. *Int J Neuropsychopharmacol* 11: 533–539, 2008. doi:10.1017/S1461145707008395.
31. **Nielsen J, Hoffert JD, Knepper MA, Agre P, Nielsen S, Fenton RA.** Proteomic analysis of lithium-induced nephrogenic diabetes insipidus: mechanisms for aquaporin 2 down-regulation and cellular proliferation. *Proc Natl Acad Sci USA* 105: 3634–3639, 2008. doi:10.1073/pnas.0800001105.
32. **Park EJ, Kwon TH.** A minireview on vasopressin-regulated aquaporin-2 in kidney collecting duct cells. *Electrolyte Blood Press* 13: 1–6, 2015. doi:10.5049/EBP.2015.13.1.1.
33. **Pham AQT, Xu LHR, Moe OW.** Drug-induced metabolic acidosis. *F1000Res* 4: F1000 Faculty Rev-1460, 2015.
34. **Poulsen SB, Kristensen TB, Brooks HL, Kohan DE, Rieg T, Fenton RA.** Role of adenylyl cyclase 6 in the development of lithium-induced nephrogenic diabetes insipidus. *JCI Insight* 2: e91042, 2017. doi:10.1172/jci.insight.91042.
35. **Rao R, Zhang M-Z, Zhao M, Cai H, Harris RC, Breyer MD, Hao C-M.** Lithium treatment inhibits renal GSK-3 activity and promotes cyclooxygenase 2-dependent polyuria. *Am J Physiol Renal Physiol* 288: F642–F649, 2005. doi:10.1152/ajprenal.00287.2004.
36. **Rej S, Herrmann N, Shulman K.** The effects of lithium on renal function in older adults–a systematic review. *J Geriatr Psychiatry Neurol* 25: 51–61, 2012. doi:10.1177/0891988712436690.
37. **Rojek A, Nielsen J, Brooks HL, Gong H, Kim YH, Kwon TH, Frøkiaer J, Nielsen S.** Altered expression of selected genes in kidney of rats with lithium-induced NDI. *Am J Physiol Renal Physiol* 288: F1276–F1289, 2005. doi:10.1152/ajprenal.00305.2004.
38. **Roy A, Al-bataineh MM, Pastor-Soler NM.** Collecting duct intercalated cell function and regulation. *Clin J Am Soc Nephrol* 10: 305–324, 2015. doi:10.2215/CJN.08880914.
39. **Schwartz GJ, Tsuruoka S, Vijayakumar S, Petrovic S, Mian A, Al-Awqati Q.** Acid incubation reverses the polarity of intercalated cell transporters, an effect mediated by hensin. *J Clin Invest* 109: 89–99, 2002. doi:10.1172/JCI0213292.
40. **Stone KA.** Lithium-induced nephrogenic diabetes insipidus. *J Am Board Fam Pract* 12: 43–47, 1999. doi:10.3122/15572625-12-1-43.
41. **Takito J, Hikita C, Al-Awqati Q.** Hensin, a new collecting duct protein involved in the in vitro plasticity of intercalated cell polarity. *J Clin Invest* 98: 2324–2331, 1996. doi:10.1172/JCI119044.
42. **Teng-umnuay P, Verlander JW, Yuan W, Tisher CC, Madsen KM.** Identification of distinct subpopulations of intercalated cells in the mouse collecting duct. *J Am Soc Nephrol* 7: 260–274, 1996.
43. **Thomsen K, Shirley DG.** A hypothesis linking sodium and lithium reabsorption in the distal nephron. *Nephrol Dial Transplant* 21: 869–880, 2006. doi:10.1093/ndt/gfk029.

44. **Trepiccione F, Capasso G, Nielsen S, Christensen BM.** Evaluation of cellular plasticity in the collecting duct during recovery from lithium-induced nephrogenic diabetes insipidus. *Am J Physiol Renal Physiol* 305: F919–F929, 2013. doi:10.1152/ajprenal.00152.2012.
45. **van Adelsberg J, Al-Awqati Q.** Regulation of cell pH by Ca+2-mediated exocytotic insertion of H+-ATPases. *J Cell Biol* 102: 1638–1645, 1986. doi:10.1083/jcb.102.5.1638.
46. **van Adelsberg J, Edwards JC, Takito J, Kiss B, al-Awqati Q.** An induced extracellular matrix protein reverses the polarity of band 3 in intercalated epithelial cells. *Cell* 76: 1053–1061, 1994. doi:10.1016/0092-8674(94)90382-4.
47. **Wall SM, Hassell KA, Royaux IE, Green ED, Chang JY, Shipley GL, Verlander JW.** Localization of pendrin in mouse kidney. *Am J Physiol Renal Physiol* 284: F229–F241, 2003. doi:10.1152/ajprenal.00147.2002.
48. **Wall SM, Lazo-Fernandez Y.** The role of pendrin in renal physiology. *Annu Rev Physiol* 77: 363–378, 2015. doi:10.1146/annurev-physiol-021014-071854.
49. **Wang Y, Klein JD, Froehlich O, Sands JM.** Role of protein kinase C-α in hypertonicity-stimulated urea permeability in mouse inner medullary collecting ducts. *Am J Physiol Renal Physiol* 304: F233–F238, 2013. doi:10.1152/ajprenal.00484.2012.
50. **Weiner ID, Verlander JW.** Renal ammonia metabolism and transport. *Compr Physiol* 3: 201–220, 2013.
51. **Wesson DE.** Endogenous endothelins mediate increased distal tubule acidification induced by dietary acid in rats. *J Clin Invest* 99: 2203–2211, 1997. doi:10.1172/JCI119393.
52. **Wesson DE, Simoni J, Green DF.** Reduced extracellular pH increases endothelin-1 secretion by human renal microvascular endothelial cells. *J Clin Invest* 101: 578–583, 1998. doi:10.1172/JCI854.
53. **Yamaji Y, Tsuganezawa H, Moe OW, Alpern RJ.** Intracellular acidosis activates c-Src. *Am J Physiol Cell Physiol* 272: C886–C893, 1997. doi:10.1152/ajpcell.1997.272.3.C886.
54. **Yao L, Huang D-Y, Pfaff IL, Nie X, Leitges M, Vallon V.** Evidence for a role of protein kinase C-α in urine concentration. *Am J Physiol Renal Physiol* 287: F299–F304, 2004. doi:10.1152/ajprenal.00274.2003.
55. **Zhang Y, Li L, Kohan DE, Ecelbarger CM, Kishore BK.** Attenuation of lithium-induced natriuresis and kaliuresis in $P2Y_2$ receptor knockout mice. *Am J Physiol Renal Physiol* 305: F407–F416, 2013. doi:10.1152/ajprenal.00464.2012.